DYNAMIC STRENGTH TESTING OF 3D-REINFORCED T-JOINTS

Manuel Herkt[*] , *Peter Middendorf*[*], *Christian Less*[**], *Werner Riedel*[***], *Georg Maier*[****] *and Klaus Drechsler*[*****]
***EADS Corporate Research Centre Germany, Dept. LG-CT, 81663 Munich, Germany,**
****EADS Miltary Aircraft, MT212, Munich, Germany,**
*****Fraunhofer Institut für Kurzzeitdynamik, Ernst-Mach-Institut (EMI), 79104 Freiburg, Germany,**
******Wehrwissenschaftliches Institut für Werk-, Explosiv- und Betriebsstoffe (WIWEB), 85435 Erding, Germany,**
*******University of Stuttgart, Institute of Aircraft Design, 70569 Stuttgart, Germany**

Keywords: *Manufacturing, Fabrication, Processing, Advanced Composite Materials, Structures*

SUMMARY

Focus of this paper is to show the performance of reinforced CRFP T-joints under dynamic loading in a specifically designed testing facility. Static strength tests have been performed as a cross reference. Samples were built out of non-crimp fabrics (NCF) and for a part of them Carbon fibres were used to reinforce the T-joints on the NCF-skin by means of a tufting-stitching head mounted on an industrial robot. These so-called preforms were then infiltrated with RTM 6 Epoxy resin and cured in an autoclave process.

The specimens were tested both dynamically and statically. Results show an increase in the ultimate strength and in the energy absorption in case of the dynamically tested samples.

1. INTRODUCTION

Structures made of high performance materials like carbon fibre reinforced plastics (CFRP) often fails in the joining area of two or more parts when loaded beyond ultimate load. This is not only true for static failure but also for dynamic loading at medium velocities like in case of crash or after-shock loading by Hydrodynamic Ram, which can be caused by objects penetrating integral tank structures.

Although there are requirements regarding safety or survivability, these specific load cases are normally not included in the design loads preventing over-sizing.

Therefore research should be focused on understanding structural behavior of joints under these specific loads to be able to find optimum joint configurations achieving damage tolerant structures. While conventionally ultimate strength of joints is considered, for damage tolerance total energy absorption is of interest. In an assembly even “weak” joints can be beneficial in giving extra degrees of freedom to the structure by failing before more important members are over-loaded.

2. TEXTILES FOR COMPOSITE APPLICATIONS

In aeronautical research projects textile technologies such as robot assisted braiding and stitching are of major interest since fibers can be placed in the direction where reinforcement is needed.

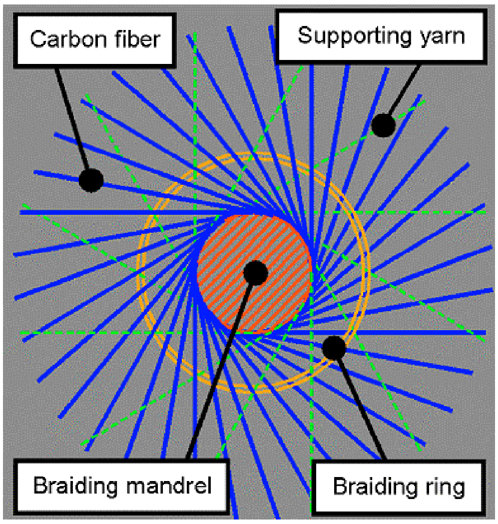

Figure 1: Schematic braiding set-up [1]

While in Figure 1 the principle setup is sketched, in Figure 2 the braiding machine as used at EADS Corporate Research Center Germany is presented.

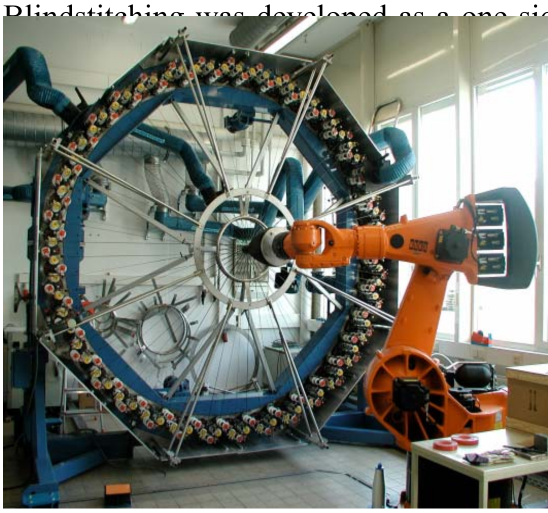

Figure 2: Robot assisted braiding in EADS Corporate Research Center, Germany

Two further interesting textile technologies for composite applications are the so called blindstitching technology and the tufting technology. In this chapter only the blindstitching will be described. Further details about tufting can be found in chapter 3.

Blindstitching was developed as a one side
is
ne
is
ng

Figure 3 shows the blindstitching head mounted on the industrial robot and the stitching process.

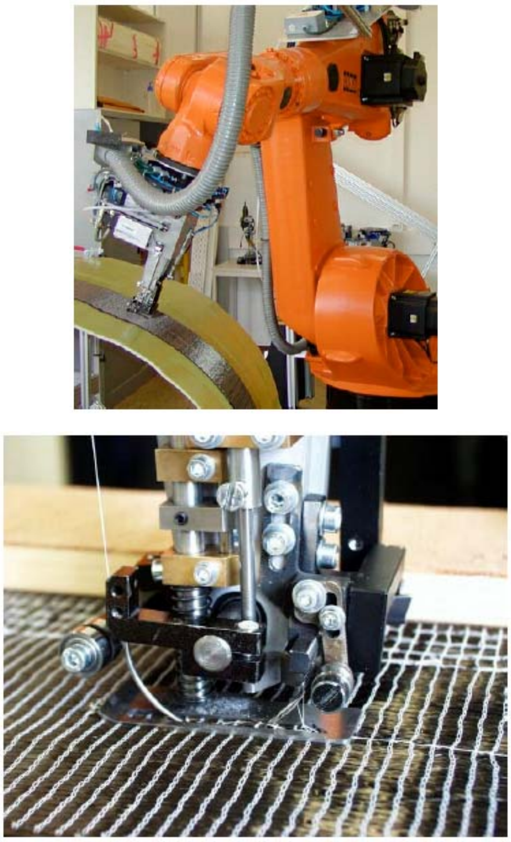

Figure 3: Blindstitching head mounted on the robot (above) and the stitching technology (below, here: use of a glass fiber as stitching yarn is shown)

Figure 4 shows the blindstitching principle. On the left hand side one can see the typically curved needle for this process and the yarn (red). The right hand side shows the stitching pattern. The principle of this technology can be described as follows: The needle stitches into the non crimp fabrics and leads the yarn on a curved trajectory through them. When exiting the material a gripper takes the yarn, creates a loop and holds it back until the needle is in the same position again.

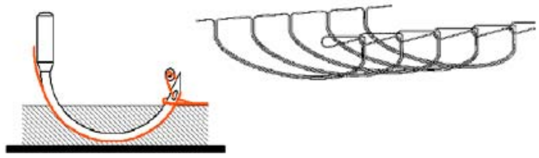

Figure 4: The blindstitching principle [2]

3. THE ROBOT ASSISTED STITCHING TECHNOLOGY AND THE MATERIAL USED

The stitching technology used for the reinforcement of the T-joints described in this paper is the so called tufting technology. This process is based on a carpet manufacturing process. The fibers are brought into the material by taking advantage of the friction forces which hold the fiber back in the material. By stitching through the material a loop is created on the lower side of it (see Figure 5 above). Figure 5 shows the tufting principle. Below one can see the second possibility which is to stitch into the material and let the loop end in it.

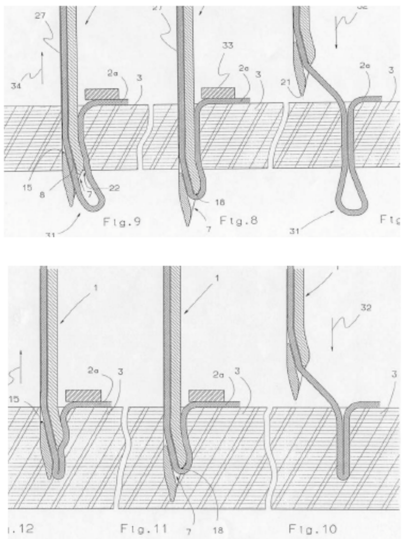

Figure 5: The tufting principle [2]

The material used had the following layup:

- [0/+45/90/-45/0/-45/90/+45/0/+45/90/-45/0/90]$_S$ for the skin
- [+45/0/-45/+45/-45/+45/0/-45]$_S$ for the spar

The noodle is a carbon fibre braid. Figure 6 shows a schematic of the textile layup for an exemplary composite T-stringer.

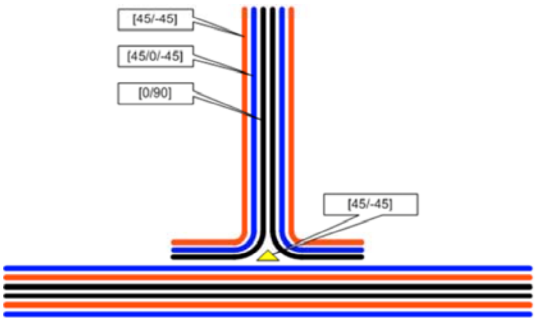

Figure 6: Schematic layup of a textile T-stringer

4. EXPERIMENTAL PROGRAMME

Basically two configurations of T-stringers were examined. The first one was not reinforced but only cured with RTM6 Epoxy resin and served as reference. The second one was reinforced by using tufting technology and carbon fibers.

The layup has been bindered for preform assembly. Again, a through-thickness reinforcement was implemented for the skin-flange connection by means of tufting with a T900-2x1k 80 tex carbon yarn. Stitch pattern was 4 x 10mm under 0° and one line each 4mm under 45° in the noodle on both flanges (see Figure 8).

Infiltration with RTM6 Epoxy resin was carried out in an autoclave process at 120°C. Nominal laminate thicknesses are 7mm for the skin and 4mm for the spar with 60% fibre volume fraction. Figure 7 shows the tooling for preform infiltration (above) and the vacuum set up (below).

Figure 7: The tooling (above) and the vacuum set up (below)

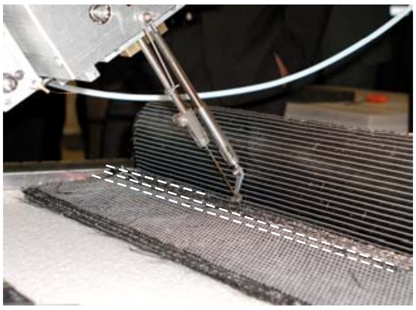

Figure 8: Tufting of the skin-flange connection (above, here: the stitches made by tufting are presented with white lines) and detailed view on the stitch pattern (below)

The dynamic strength testing has been performed in a specially designed test facility at EMI (see Figure 9.)

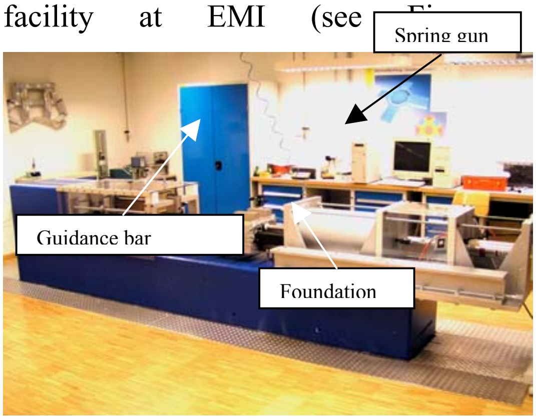

Figure 9: The test facility at EMI

The test facility's testing principle is as follows:

An air bearing sledge is accelerated by a hydraulically compressed spring. The power transfer from the spring to the sledge is done by a pusher bar, which is guided within a cylindrical pipe. The sledge collides with the mounting device of the sample and causes well-defined rupture of the specimen. Acceleration of the sledge is realised in terms of a strong helical spring with a spring constant 700 kN/m and maximum spring travel of 200 mm, pre-stressed by means of a hydraulic cylinder. Maximum available crash energy is about 4500 J [3].

Figure 10 shows the sample mounting system and the arrangement of the individual components of the measurement technique in the test setup. In Figure 11 a detailed view of the sample mounting system is shown.

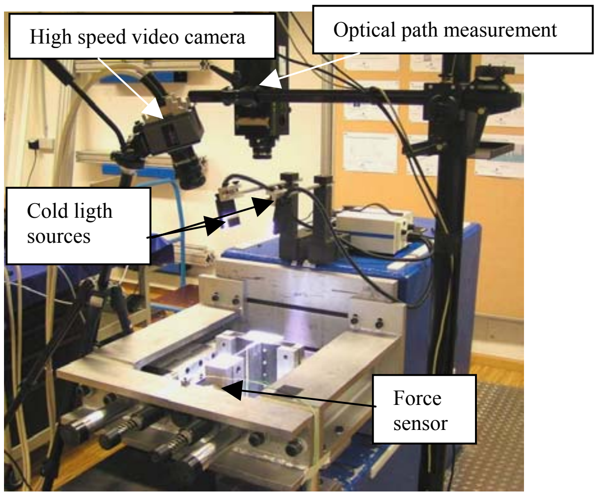

Figure 10: Arrangement of the measurement technique

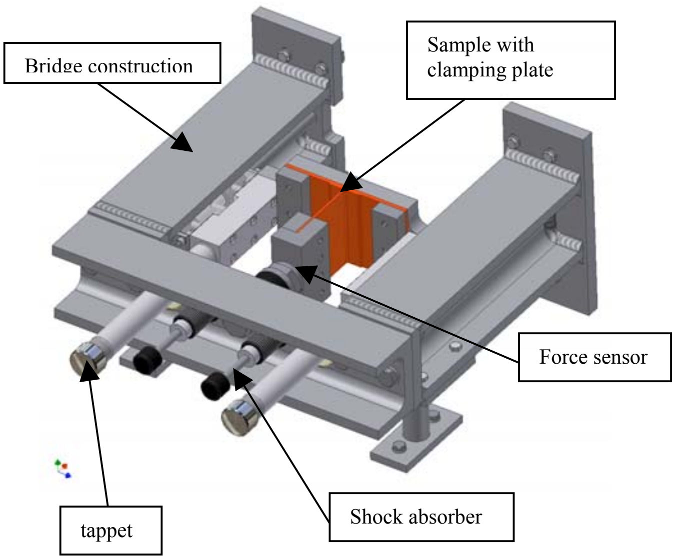

Figure 11: Entire sample mounting system

5. RESULTS

The two T-stringer configurations described in chapter 4 have been tested dynamically. Results showed that for specimens reinforced by tufting an increase of peak forces of about 100 % in the force-displacement diagram can be seen.

Furthermore tests to determine the energy absorption of the joints have been carried out. As one can see in Figure 9 below, an increase in the energy absorption of the reinforced samples of about 140 % can be detected. The maximum force levels of unreinforced samples amount to the range between 12.8 and 15.4 kN, except for sample 3.6 (see Figure 12). Peak forces are reached after an average failure deformation of 3 mm. The values obtained for total failure deformation are between 4.5 and 6 mm. The variance of the measurement data is considerably lower compared to the test series with reinforced samples. The total failure displacement is already known from the force-displacement diagram. For this sample type it amounts to approx. 4.5 - 6 mm. This is also the relevant range for determining the energy absorption. For eight out of nine samples the energy absorption until failure of the joint amounts to approximately 32 - 40 J.

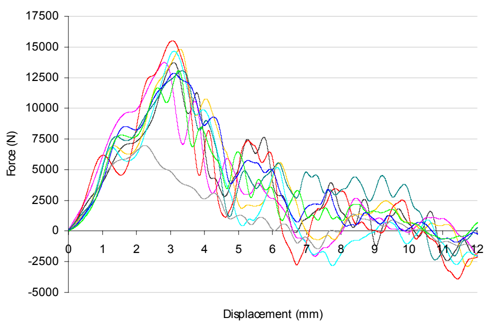

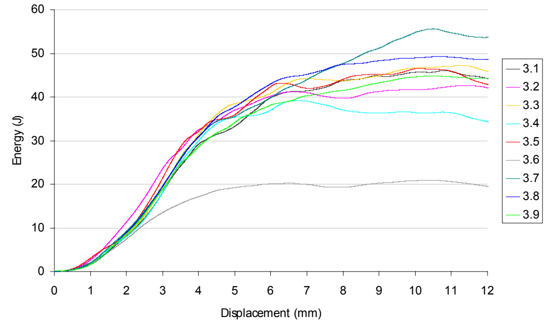

Figure 12: Ultimate strength (above) and energy absorption (below) of the dynamically tested unreinforced specimens [3]

As one can see in Figure 13 the maximum force of the reinforced samples ranges from 20 to 30kN. The force maximum is reached after failure deformation of approx. 5 mm. The average failure displacement amounts to between 5.5 and 7.5 mm. Five out of nine samples (2.1, 2.2, 2.3, 2.6, and 2.7) show a higher force level of 28-30 kN compared to the other samples. Samples 2.8 and 2.9 show a noticeable behaviour: The force maximum of about 20 kN is already reached after a displacement of 3.5 mm. Complete failure occurs after a displacement of 5.5 mm. This observed variability could be derived from the manufacturing process

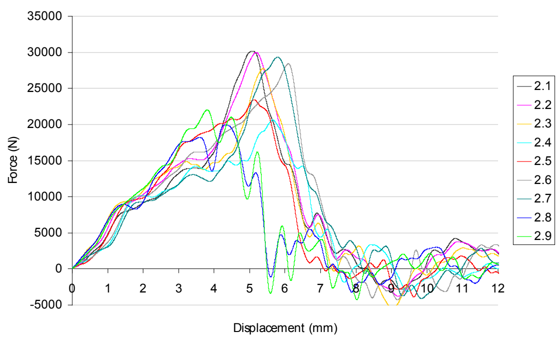

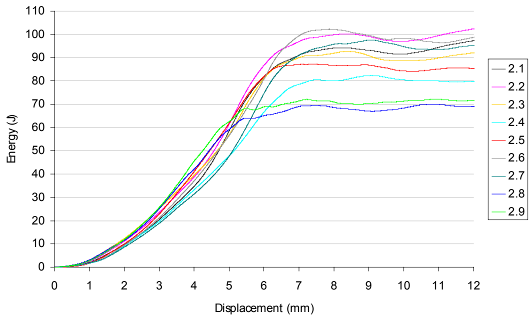

Figure 13: Ultimate strength (above) and energy absorption (below) of the dynamically tested reinforced specimens [3]

As a cross reference static strength tests of reinforced and unreinforced CFRP T-joints by means of T-pull testing have been performed by WIWEB (see Figures 15 to 17). The principle of the T-pull test is shown in Figure 14.

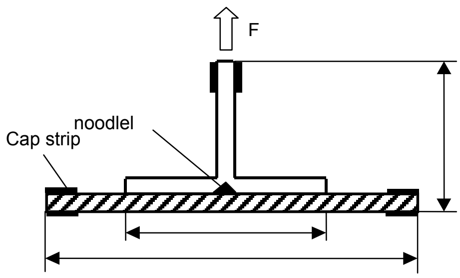

Figure 14: Principle of the T-pull test [2]

The results of these tests are presented below.

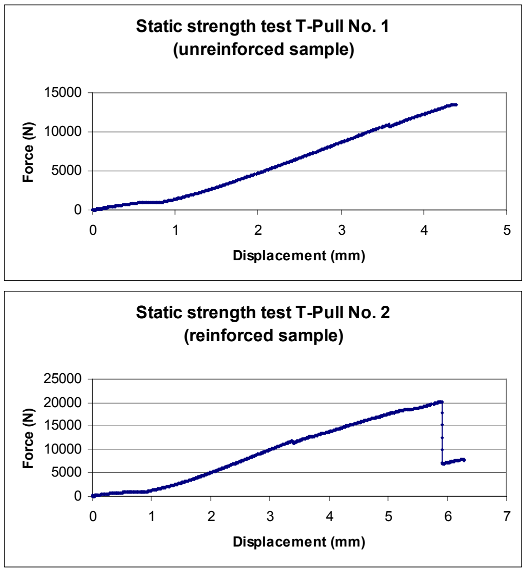

Figure 15: Testing couple of an unreinforced (above) and and a reinforced (below) CFRP T-joint

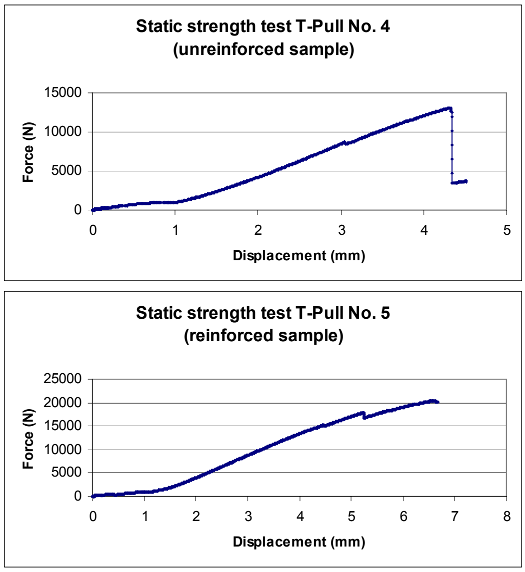

Figure 16: Testing couple of an unreinforced (above) and and a reinforced (below) CFRP T-joint

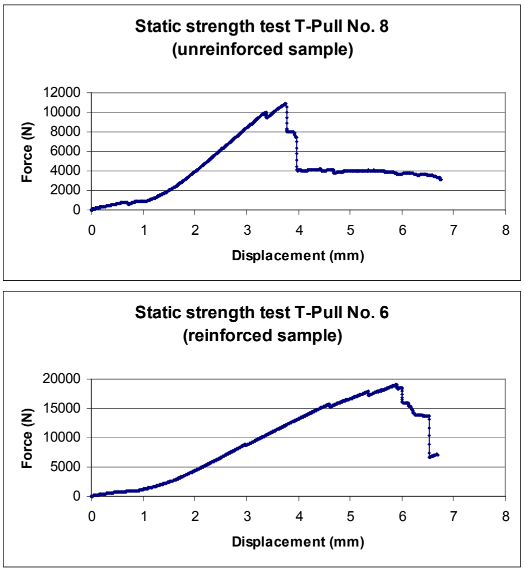

Figure 17: Testing couple of an unreinforced (above) and and a reinforced (below) CFRP T-joint

By comparing the unreinforced samples 1, 4 and 8 the mean value of the residual strength can be given as 12506,6 N. The mean value of the reinforced samples can be given as 19874 N.

This indicates an increase in loading capacity of about 59 %. Together with higher deformability at peak load, an increase in dynamic toughness by about 100% is reached.

Interestingly the reinforced samples show strain rate sensitivity with loading capacities rising by at least 25% in most test cases. This kind of dependence is not observed for the unreinforced samples underlining the change in deformation mechanisms between the two joint types.

6. CONCLUSION AND OUTLOOK

It has been shown that reinforcing of complex CFRP structures by means of robotic stitching leads to a significant increase of resistance and energy absorption of the material. These results –especially the energy absorption– gives important information about the toughness of the connection area. Furthermore a test facility has been described by with it was possible to test aircraft structures dynamically.

ACKNOWLEDGEMENTS

The authors would like to thank Christian Metzner for performing the layup and the curing of the T-stringers. The contributions by Sven Guth and Joachim Hauber on the dynamics pull tests are gratefully acknowledged.

LITERATURE

[1] A. Geßler, J. Brandt, F. Maidl, C. Breu, J. Horn, H. Schneider, *Neue Entwicklungen bei der Fertigung von Kohlenstofffaserpreforms mit der Rundflechttechnik*, Deutscher Luft- und Raumfahrtkongress, Dresden, September 20-23, Dresden, Germany

[2] *Textile Integrationstechniken zur Herstellung vorkonfektionierter Verstärkungsstrukturen für FVK „INTEX“*, Förderkennzeichen 03N3060A9

[3] EUCLID-RTP-3.32 Low Vulnerability Composite Structures for Military Aircraft, *Initial Report on Test and Evaluation of Coupons and Details*, RTP-3.32/6A-1/TR/EMI/I-44-05/Issue (A), EMI-Report I-44-05, 2005